Image Fusion for optimizing Gamut Mapping

Peter Zolliker[1)]***, Zofia Barańczuk***[1)]***, and Joachim Giesen***[2)]
[1)] ***Laboratory for Media Technology; Swiss Federal Laboratory for Materials Testing and Research (Empa), Dübendorf, Switzerland***
[2)] ***Friedrich-Schiller-Universität Jena, Germany***

Abstract

In this paper we study a local, image dependent approach to the gamut mapping problem. A structural image quality measure is used to pick an optimal mapping algorithm for image patches from a given class of algorithms. The optimally mapped patches are then fused into a single mapping of the image. We discuss and compare two image fusion methods that are designed to avoid artifacts in the fused image. Psycho-visual experiments confirm that this approach has a good potential to obtain mapped images with higher perceived quality than any of the individual algorithms, on which the method is based.

INTRODUCTION

The rendering of a color image constrained by device limitations, also called gamut mapping, is a classical problem in digital color reproduction and still an active area of research, see [1, 2] for an overview. In recent years, research on gamut mapping algorithms (GMAs) has focused (1) on spatial mapping algorithms that map each pixel in an image, depending individually on its neighborhood [3, 4, 5, 6], and (2) on image dependent algorithms where the mapping take image's inherent color distribution into account [7, 8]. Another successful approach towards image dependence has been published recently [9]: given a finite number of gamut mapping algorithms and a suited similarity measure for an image, the mapping algorithm that produces the mapping most similar to the original image is chosen.

In this paper we study methods to take this approach one step further, namely applying it locally to patches of the image or even to individual pixels and then fusing the optimally mapped patches into a global mapping. The success of such a method will depend mainly on two factors: (1) a good measure to determine the optimal gamut mapping algorithm for an image patch or even more generally for every pixel, and (2) an image fusion technique to combine the mapped patches/pixels into one image of high perceptual quality.

Image quality measures have been successfully used in many imaging applications, e.g., in modeling image distortions, especially in data compression. An overview of the state-of-the-art in image quality research can be found in [10] or [11]. A special class of image quality measures that play an important role in the evaluation of sophisticated gamut mapping algorithms measures the structural similarity of images, and hence can be used for comparing modified images with their originals. Among these measures is the frequently used *Structural Similarity Index Measure (SSIM)* that has been introduced in [12].

Image fusion is the process of combining two or more images of the same object into one extended composite image [13]. In general, several problems have to be solved for successful image fusion: registration, matching dynamic range, and smooth, artifact-free combination. Typical applications of image fusion are the construction of high dynamic range (HDR) images based on a set of exposures [14], or the combination of IR-images with visual color images [15]. The first approach using image fusion in the domain of gamut mapping has been published by [16]. In gamut mapping registration is not a critical issue. The challenge here is the smooth and artifact-free transition between regions mapped by different algorithms.

The goal of this paper is to explore the feasibility of locally optimal gamut mapping using image quality measures and image fusion. Here we use an extended version of SSIM as image quality measure and investigate two methods for the image fusion part. The results are judged and compared in a psycho-visual test.

METHODOLOGY

General concept

Conceptually, we devise a meta-algorithm which selects for every image pixel of an original image O an optimal mapping from a set of basic gamut mapping algorithms $GMA_i, i = 1,\ldots,n$. The meta-algorithm comprises the following three steps:

(1) All pixels of the original image O are mapped by all gamut mapping algorithms GMA_i.
(2) For every pixel the optimal mapping is selected by optimizing the similarity between the neighborhood of the original and the mapped pixel. The result is a set of n similarity maps Sim_i describing the similarity between the original patch centered at pixel j and its mapping with GMA_i. Note that this means that Sim_i assigns a similarity score to every pixel for the algorithm GMA_i.
(3) An image fusion method is used to combine the optimally mapped pixels into a single smooth image R. The main challenge here is to avoid artifacts at patch boundaries, or more generally image parts, that have been mapped with different gamut mapping algorithms.

In this paper we focus on the third step of the of meta-algorithm, the image fusion. For the first two steps we use state-of-the-art gamut mapping algorithms and an extended version of the structural similarity image measure SSIM [12]. We also restrict ourselves to pixel centered neighborhoods that provide us with similarity maps $Sim_i, i = 1,\ldots,n$ for every base algorithm. The meta-algorithm is summarized in Figure 1.

In particular, we study two fusion techniques, one based on image segmentation and the other based on a bilateral filter. Details are described in the following three subsections.

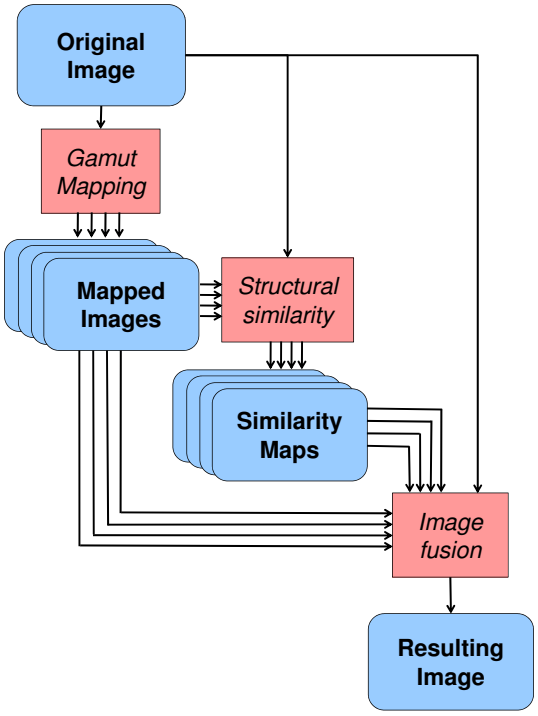

Figure 1. *General concept of the construction of a meta algorithm using a set of basic gamut mapping algorithms*

Gamut Mapping Algorithms

For this paper we chose four gamut mapping methods to serve as base algorithms. Note, that the focus here is not to include or exclude a specific algorithm. The importance for the potential success of the fusion method is, that the chosen algorithms, though different from each other, provide overall comparable perceived quality. The chosen algorithms, that all go beyond pixel-wise mapping and include some spatial mapping features, are the following (the first two are based on the reference algorithms described in the guidelines for the evaluation of gamut mapping algorithms [17] with subsequent contrast recovery [4]):

- GMA_1: Hue preserving minimum distance clipping (HPMinDE) using CIELAB as working color space with subsequent contrast recovery.
- GMA_2: Chroma-dependent sigmoidal lightness mapping and cusp knee scaling (SGCK) using IPT [18] as working color space with subsequent contrast recovery.
- GMA_3: An implementation of the multilevel algorithm [6] using CIELAB as working color space. This algorithm is based on mapping different frequency bands of the images. Special emphasis is put on hue preservation and the avoidance of artifacts (halos) and over-compression.
- GMA_4: An algorithm [19] using IPT as working color space, that first performs a chroma-dependent gray axis transform. The input image is then split into a low frequency and a high frequency part using a Gaussian filter. The low frequency part is clipped to the target gamut, and then the high frequency part is added back. The result is clipped again to ensure that all colors are in the target gamut.

Structural Similarity

We determine the optimal mapping for an pixel from its neighborhood (here 9×9 pixel centered patches) using a structural image similarity measure, providing us with a similarity map Sim_i for every base mapping algorithm GMA_i (see Step 2 of the meta-algorithm). The structural image similarity measure is an extension of the SSIM measure which is defined for one channel only, typically the lightness channel, and consists of two basic factors, one responsible for average lightness differences, and the other for contrast and structural differences. However, we also want to have the possibility to consider color related similarities in particular hue. Therefore we extend the SSIM measure by an additional factor for hue shifts. We do not consider structural correlations in hue since the perception of structural information is mainly governed by lightness. In order to derive a meaningful hue measure, a hue preserving color space has to be used. Here we use the IPT color space [18] which is known to have good hue preserving properties. Hence, we apply the standard SSIM formula to the lightness coordinate I of the IPT color space. The standard SSIM formula [12] reads as follows (note that x always refers to pixels in the original image and y to pixels in the mapped image):

$$SSIM(x,y) = \frac{(2\mu_x\mu_y + c_1)(2\sigma_{xy} + c_2)}{(\mu_x^2 + \mu_y^2 + c_1)(\sigma_x^2 + \sigma_y^2 + c_2)}, \tag{1}$$

where μ_x is the average of the luminance values I in the patch centered at x, σ_x is the standard deviation of these values, σ_{xy} is the correlation between luminance values in the patch centered at x (before mapping) and the values in the patch centered at y (after mapping), and c_1 and c_2 are constants. For hue differences we use the following similarity factor

$$h(x,y) = \frac{1}{c_3 \cdot \Delta H(x,y)^2 + 1} \tag{2}$$

with constant c_3. In the IPT color space hue differences ΔH can be calculated from the chroma coordinates P and T as follows:

$$\Delta H = \sqrt{(P_x - P_y)^2 + (T_x - T_y)^2 - \Delta C^2} \quad , \tag{3}$$

where

$$\Delta C = \sqrt{P_x^2 + T_x^2} - \sqrt{P_y^2 + T_y^2}. \tag{4}$$

The extended structural similarity measure now assigns to every pixel x in the original image and pixel y in the mapped image the following similarity score

$$SSIM^+(x,y) = SSIM(x,y) \cdot h(x,y). \tag{5}$$

The parameters $c_1 = 1.0$ and $c_2 = 9.0$ are chosen as in [12]. The parameter $c_3 = 0.05$ is optimized on an image with many saturated blue colored pixels. Since we can assume, that all base gamut mapping algorithms optimize chroma in similar ways, it seems not appropriate to introduce also a chroma factor in the similarity measure.

Using the $SSIM^+$ measure we obtain four similarity maps Sim_i, one for each of the base mapping algorithms. Figure 2 shows an example of the four (scaled) similarity maps.

Figure 2. *Similarity maps Sim_i for the for four base algorithms $GMA_i, i = 1,\ldots,n$. At light pixels the similarity is high, and at dark pixels the similarity is low. To improve the readability of the visualization the lightness of the images has been scaled.*

Image fusion

The most simple approach to image fusion in our setting would be to map every pixel j with the algorithm $GMA_i, i \in \{1,\ldots,4\}$ such that

$$i = \text{argmax}_{k=1,\ldots,4} sim_{kj} \tag{6}$$

where sim_{kj} is the value for pixel j in the similarity map Sim_k.

However, this approach results in unwanted artifacts. A typical example for an image resulting from this fusion approach is shown in Figure 4 (top). Hence, the challenge is to find a better fusion scheme that avoids such artifacts, but still provides a close to optimal mapping in every part of the image. In the following, we describe two fusion schemes, one based on segmentation, and the other based on bilateral filtering of weighted maps computed from the similarity maps.

Segmentation

The image fusion process using segmentation is summarized in Figure 3. Input to the segmentation based fusion algorithm are the similarity maps Sim_i for the mapping algorithms GMA_i that assign a similarity score to every pixel of the image O that has to be mapped, and a state-of-the-art image segmentation method that will be applied to O. For the segmentation we use an implementation[1] of the algorithm described by [20]. This algorithm has three parameters that we need to set: (1) a parameter σ that controls a smoothing of the input image before segmentation, (2) a value k that is used for thresholding, and (3) the minimum component size min enforced in a post-processing step. We use the following parameter settings $\sigma = 0.5$, $k = 500$ and $min = 1000$. Note that the value for min was chosen higher than the recommended default value because for us it is important to avoid very small segments.

From the similarity maps an index map can be computed that assigns to every pixel in O the index of the mapping algorithm that achieves the highest similarity score on this pixel. See the top right image in Figure 3 for a visualization of an index map, where the index values have been encoded by grey level values.

[1] see http://people.cs.uchicago.edu/~pff/segment/

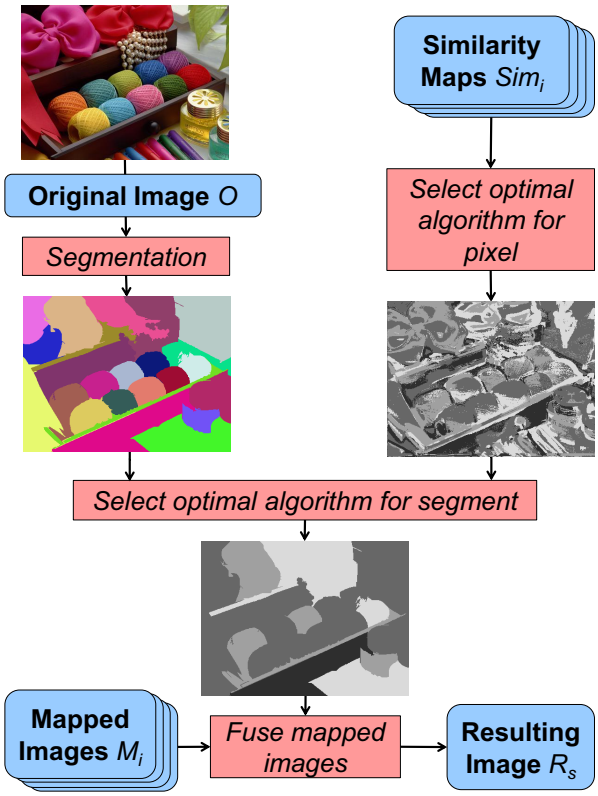

Figure 3. *Fusing mapped images based on a segmentation of the original image.*

The top left image in Figure 3 shows the segmentation of the original image O, where the different segments have been encoded by different colors. For every segment in the segmentation of O we select the algorithm GMA_i such that the majority of the pixels in this segment are mapped by the index map to index i, i.e., GMA_i achieves the highest similarity score on more pixels of the segment than any other mapping algorithm (where ties are broken arbitrarily). This results in a smoothed index map—an example is shown in the image at the bottom of Figure 3.

A typical result of the mapping process after image fusion using the segmentation approach and the similarity maps for our four base algorithms is shown in the bottom image in Fig. 4. Note that the artifacts induced by the naive fusion scheme (see top image in Fig. 4) have vanished.

Bilateral Filter

The image fusion process using a bilateral filter is summarized in Figure 5.

In the segmentation approach we use an index map that assigns exactly one—the winning—index to every pixel. Now we want to consider all mappings at every pixel by weighting their influence using the similarity maps Sim_i for the mapping algorithms $GMA_i, i = 1,\ldots,n$. Let

$$\mu_j = \frac{1}{n}\sum_i sim_{ij}. \tag{7}$$

be the average similarity score of the mapping algorithms at pixel j computed on a patch centered at j. We define a weighting map

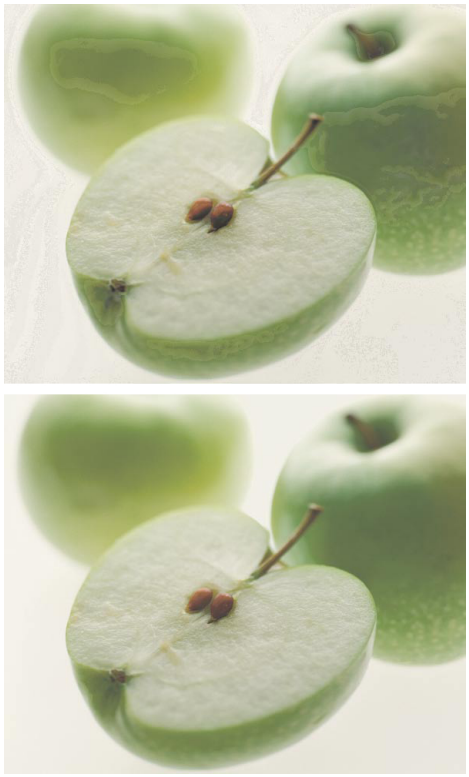

Figure 4. *Fused image based on the segmentation approach (bottom) compared to fusion without smoothing (top)*

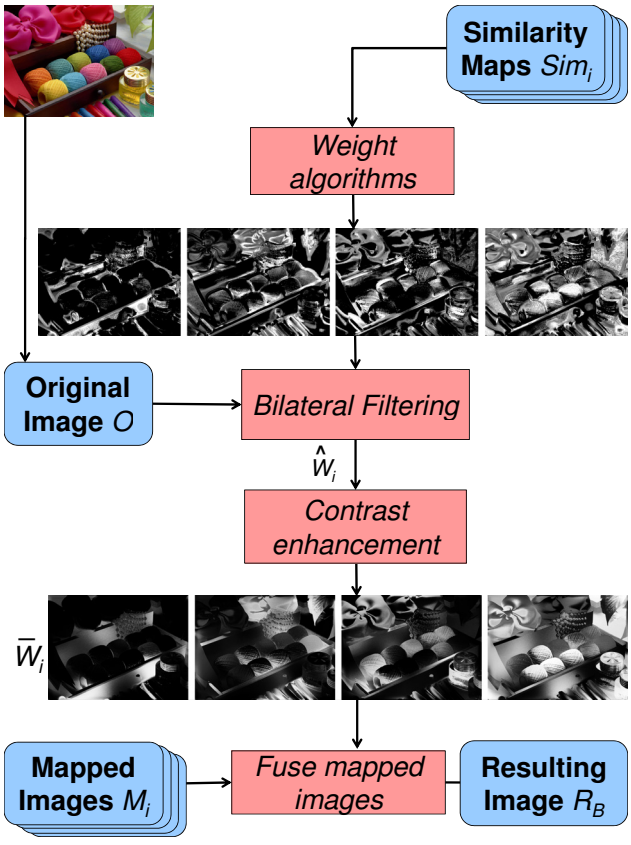

Figure 5. *Fusing mapped images using bilateral filtering.*

W_i for every mapping algorithms GMA_i that assigns to every pixel j the weight w_{ij} that is given as follows

$$w_{ij} = \frac{\max(sim_{ij} - \mu_j, 0)}{\sum_{k=1}^{n} \max(sim_{kj} - \mu_j, 0)}, \tag{8}$$

i.e., all similarity scores below μ_j are set to zero and the sum of the weights for the different mapping algorithms at pixel j are normalized to 1. Typical weighting maps are shown as images in the top row of Figure 5.

In a next step the weighting maps W_i are smoothed by using a bilateral filter resulting in smoothed weighting maps $\hat{W}_i$ that assign the following weight to pixel j,

$$\hat{w}_{ij} = \frac{\sum_k w_{ik} \cdot f_{jk}}{\sum_k f_{jk}}. \tag{9}$$

Here f_{jk} is a bilateral filter kernel of the form

$$f_{jk} = e^{-((\Delta^S_{jk}/\sigma_s)^2 + (\Delta^C_{jk}/\sigma_c)^2)}, \tag{10}$$

where Δ^S_{jk} is the spatial distance of the pixels j and k, Δ^C_{jk} is their color distance in the original image, and σ_s and σ_c are parameters defining a spatial reference distance and a color reference distance, respectively. In our experiments we use $\sigma_s = 5\%$ of the image diagonal and $\sigma_c = 20$.

Finally, in order to increase the separation of the different mapping algorithms the smoothed weights are modified once more by increasing the global contrast as follows

$$\bar{w}_{ij} = \frac{\tanh(g_c \cdot \tanh^{-1}(2\hat{w}_{ij} - 1)) + 1}{\sum_{k=1}^{n} \tanh(g_c \cdot \tanh^{-1}(2\hat{w}_{kj} - 1)) + 1}, \tag{11}$$

where g_c is a parameter that controls the amount of contrast enhancement. In our experiments we use $g_c = 2$. This results in contrast enhanced weighting maps $\bar{W}_i$ for every mapping algorithm GMA_i. Typical weighting maps $\bar{W}_i$ are shown in the images in the bottom row of Figure 5.

The weighting functions $\bar{W}_i$ can now be used in a straightforward manner to fuse the images obtained from the different mapping algorithms by interpolating the different mappings pixelwise using the weights $\bar{w}_{ij}$.

EXPERIMENT

Test Setup

In order to test the visual performance of the meta-algorithm and especially the two fusion schemes that we have discussed before, we have set-up a psycho-visual test with the following properties:

Test method. We used a pair comparison test where an original image and two mapped images were presented to an observer. For every pair comparison the orignal image and simulation of two mapped images were shown on the same screen. The observers had to select the mapped image that represents the original image better. An observer could also state, that both mapped images were equally good.

Laboratory setup. The test images were shown on a 22" Eizo CG 220 LCD monitor that had been calibrated to show sRGB-colors. The luminance of the monitor white was $120cd/m^2$ and the ambient light at $20-40lx$. Monitor flaps around the

screen were used to prevent flare. The monitor's background was set to a neutral gray.

Image selection. We used an image set that contains images representing a wide variety of natural scenes. The image set also included the obligatory ski image as specified in the CIE 156:2004 guidelines [17]. In total 36 different images were used in the experiment. One of the images was excluded from the final evaluation, because it was used to optimize the hue parameter for the $SSIM^+$ measure (see the earlier discussion of the $SSIM^+$ measure). The images from the test set are shown in Figure 6.

Figure 6. *Test images*

Observers. Ten observers (four female and six male) participated in the test. All observers had passed the Ishihara test for color deficiencies. The observers participated in four to six test sessions each consisting of 90 comparisons. All in all 5130 comparison have been made.

Algorithms. The following mapping algorithms were compared: the four base algorithms GMA_1, GMA_2, GMA_3, GMA_4, and two instances of our meta-algorithms based on the two different image fusion schemes $Fusion_S$ (segmentation) and $Fusion_B$ (bilateral filter). For the test, we used a work-flow for mapping images from sRGB to offset CMYK on uncoated paper[2]. The choice of a rather small target gamut provides us with significant, visible differences among the four base algorithms, and such that artifacts induced by the image fusion step should be perceptually more significant than for larger target gamuts.

Computational complexity. The computation time of the fusion process itself is comparable to that of a typical single algorithm in our set of base algorithms. The main task is a bilateral filter (as in GMA_1 or GMA_2) or a segmentation method. Thus for our selection of base algorithms the total computation time is about five time that of an average single GMA. Note that an optimization of computation time was not the primary issue of this research.

Results

The visual performance of an additional meta-algorithm [9] Max_{SSIM^+} was computed from the user data. This algorithm picks the best base algorithm for an image using the structural similarity measure $SSIM^+$. The data were evaluated using Thurstone's Case V model [21]. Results are shown in Figure 7. The error bars indicate one estimated standard deviation.

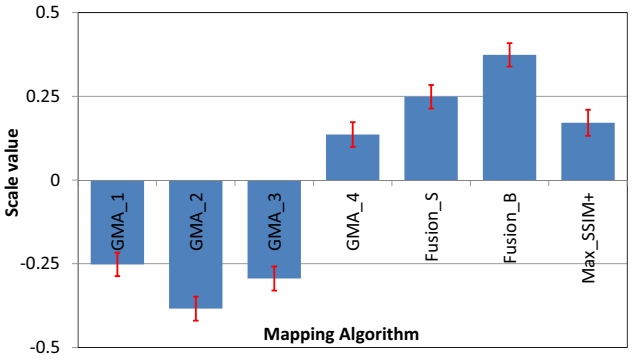

Figure 7. *Psycho-metric scaling results showing relative performance of the four base and the three meta-algorithms. The error bars indicate one estimated standard deviation.*

The result shows that generally the three meta-algorithms $Fusion_S$, $Fusion_B$ and Max_{SSIM^+} perform better than the four base algorithms. The results for Max_{SSIM^+} are in line with the results that have been published in [9]. The performance of the segmentation based fusion technique $Fusion_S$ is slightly better than that of Max_{SSIM^+}, but this result is not statistically significant. The bilateral filter based fusion technique $Fusion_B$ performed best and this is a statistically significant improvement over each of the four base algorithms.

DISCUSSION

The results of our psycho-visual test show that locally optimized gamut mapping has the potential for significant improvements of gamut mapping algorithms. Even if one of the base algorithms performed significantly better than the other three, a closer look into the data revealed that any of the four base algorithms obtained above average psycho-metric scale values for at least one of the test images. The same is true, if the algorithms are judged using $SSIM^+$ as a measure. Hence, we can assume that every base algorithm had a positive contribution to the images mapped with the meta-algorithm.

The presented meta-algorithm performed well in our test but it is still far from being optimal. Potential for further improvements can be found in all three steps, (1) the selection of the base mapping algorithms, (2) the structural similarity measure, and (3) the fusion method.

Especially, the structural similarity measure needs more attention for further improvement of the gamut mapping quality. The presented measure is far from being perfect: the parameters to control the hue deviation were optimized only at a very basic level and chroma deviations were not considered. The role of hue and chroma preservation in extensions of the SSIM structural similarity measure is still an open research question, as is the question whether it is sufficient to consider structural information only on

[2]Using the ICC-Profile 'Isouncoatedyellowish.ICC' from `www.eci.org`

the lightness channel.

Note, that the goal of finding a perfect measure is probably unattainable. If such a measure would be known, a gamut mapped image could in principle be optimized directly by optimizing this measure, however most likely by incurring large computational costs. Hence, it is still interesting to manually investigate optimized gamut mapping algorithms in combination with incomplete similarity measures for further improving gamut mapping.

Both fusion techniques that were discussed have the potential for further improvement. One weakness of the segmentation technique is that in some images artifacts are visible when the segmentation does not match with a natural segmentation of an image. If such images could be detected automatically—for example using an appropriate automatic artifact detector—the performance of the mapping algorithm could be improved.

Finally, some of the parameters in the bilateral filtering technique can be optimized further. In particular, the contrast enhancement parameter g_c is critical. A small value (close to 1) tends to average out the algorithms, thus tending to produce also only average quality. A high value on the other hand will produce artifacts because the transition from one algorithm to another algorithm may not be smooth anymore, especially in image regions with no clear edges.

The strength of the presented concept is, that even with an imperfect similarity measure and a set of simple base mapping algorithms the fused mapping of images provides a significant improvement of the perceived mapping quality.

CONCLUSIONS

We have shown that the fusion of locally optimal gamut mapped images has the potential to increase the perceived quality of the mapped images significantly. Further improvements can be expected for both, the selection of an optimal mapping for an image region as well as for the optimization of the image fusion technique.

In this work we used a similarity measure to select an optimal mapping for an image region, however, the selection could also be based on a large data base of suitable user preference data.

Another direction of future research could be optimizing the parameters employed in the fusion techniques based on the quality measure that has been used for the local selection of the base gamut mapping algorithm.

The proposed fusion techniques can be applied also to other imaging problems such as locally optimized image enhancement. In the latter application the set of base mapping algorithms would be replaced by a set of image enhancement algorithms and the structural similarity measure by a non-reference image quality measure.

ACKNOWLEDGEMENTS

This research was financially supported by the Hasler Foundation Proj. # 2200.

References

[1] J. Morovic. *Colour Gamut Mapping*. WileyBlackwell, ISBN 0470030321, 2008.

[2] Z. Barańczuk, J. Giesen, K. Simon, and Zolliker P. *Advances in Imaging and Electron Physics*, volume 160, chapter Gamut Mapping, pages 1–34. edited by Peter. W. Hawkes, Elsevier, 2010.

[3] R. Kimmel, D. Shaked, M. Elad, and I. Sobel. Space-dependent color gamut mapping: a variational approach. *IEEE Transactions on Image Processing*, 14(6):796–803, 2005.

[4] P. Zolliker and K. Simon. Retaining local image information in gamut mapping algorithms. *IEEE Transactions on Image Processing*, 16(3):664–672, March 2007.

[5] N. Bonnier, F. Schmitt, M. Hull, and Leynadier C. Spatial and color adaptive gamut mapping algorithms. In *Color Imaging X: Processing, Hardcopy and Applications*, volume 15, pages 267–272, Scottsdale, AR, 2007. IS&T/SID.

[6] I. Farup, C. Gatta, and A. Rizzi. A multiscale framework for spatial gamut mapping. *IEEE Transactions on Image Processing*, 16(10):2423–2435, October 2007.

[7] H. Kotera and R. Saito. Compact description of 3-d image gamut by r-image method. *Journal of Electronic Imaging*, 12(4):660–668, October 2003.

[8] A. Golan and H. Hel-Or. Novel workflow for image-guided gamut mapping. *Journal of Electronic Imaging*, 17(3):033004–1–11, July 2008.

[9] Z. Barańczuk, P. Zolliker, and J. Giesen. Image-individualized gamut mapping algorithms. *Journal of Imaging Science and Technology*, 54(3):Article number 030201 (7 pp.), May/June 2010 2010.

[10] B. Keelan. *Handbook of Image Quality*. Marcel Dekker, Inc., 2002.

[11] J. Dijk. *In search of an Objective Measure for the Perceptual Quality of Printed Images*. PhD thesis, Delft University of Technology, 2004.

[12] Z. Wang, A.C. Bovik, H.R. Sheikh, and E.P. Simoncelli. Image quality assessment: From error visibility to structural similarity. *IEEE Transactions on Image Processing*, 13(4):600–612, April 2004.

[13] H. B. Mitchell. *Image Fusion, Theories, Techniques and Applications*. Springer Verlag, Heidelberg, Germany, 2010.

[14] S. Battiato, A. Castorina, and M. Mancuso. High dynamic range imaging for digital still camera: an overview. *Journal of Electronic Imaging*, 12(3):459–469, July 2003.

[15] Clément Fredembach and Sabine Süsstrunk. Colouring the near infrared. In *Proceedings of the IS&T/SID 16th Color Imaging Conference*, pages 176–182, 2008.

[16] Y. Wang, P. Zeng, and X. Luo. Color gamut mapping based on image fusion. In *International Conference on Computer Science and Software Engineering*, pages 801–805. IEEE Computer Society, 2008.

[17] CIE. *CIE Publication 156: Guidelines for the Evaluation of Gamut Mapping Algorithms*. Central Bureau of the CIE, Vienna, 2004.

[18] Fritz Ebner and Mark D. Fairchild. Developement and testing of a color space (IPT) with improved hue uniformity. *Proceedings of 6th IS&T/SID Color Imaging Conference, Scottsdale AZ*, pages 8–13, 1998.

[19] M. Meili, D. Küpper, Z. Barańczuk, U. Caluori, and K. Simon. Filter methods to preserve local contrast and to avoid artifacts in gamut mapping. In *Color imaging XV: Displaying, Processing, Hardcopy, and Applications*, page 77280I(12pp.), San Jose, CA, 2010. SPIE/IS&T.

[20] P. F. Felzenszwalb and D. P. Huttenlocher. Efficient graph-based image segmentation. *IEEE Transactions on Image Processing*, 59(2):167–181, September 2004.

[21] Peter G. Engeldrum. *Psychometric Scaling, A Toolkit for Imaging Systems Development*. Imcotek Press, Winchester MA, USA, 2000.

